

## Increased YAP Activation Is Associated With Hepatic Cyst Epithelial Cell Proliferation in ARPKD/CHF

Lu Jiang,\* Lina Sun,\*<sup>1</sup> Genea Edwards,\* Michael Manley Jr.,\* Darren P. Wallace,†‡  
Seth Septer,§<sup>2</sup> Chirag Manohar,\* Michele T. Pritchard,\*‡ and Udayan Apte\*‡

\*Department of Pharmacology, Toxicology and Therapeutics, University of Kansas Medical Center, Kansas City, KS, USA

†Department of Internal Medicine, University of Kansas Medical Center, Kansas City, KS, USA

‡The Jared Grantham Kidney Institute, University of Kansas Medical Center, Kansas City, KS, USA

§Department of Gastroenterology, Children's Mercy Hospital, Kansas City, KS, USA

Autosomal recessive polycystic kidney disease/congenital hepatic fibrosis (ARPKD/CHF) is a rare but fatal genetic disease characterized by progressive cyst development in the kidneys and liver. Liver cysts arise from aberrantly proliferative cholangiocytes accompanied by pericystic fibrosis and inflammation. Yes-associated protein (YAP), the downstream effector of the Hippo signaling pathway, is implicated in human hepatic malignancies such as hepatocellular carcinoma, cholangiocarcinoma, and hepatoblastoma, but its role in hepatic cystogenesis in ARPKD/CHF is unknown. We studied the role of the YAP in hepatic cyst development using polycystic kidney (PCK) rats, an orthologous model of ARPKD, and in human ARPKD/CHF patients. The liver cyst wall epithelial cells (CWECs) in PCK rats were highly proliferative and exhibited expression of YAP. There was increased expression of YAP target genes, *Ccnd1* (cyclin D1) and *Ctgf* (connective tissue growth factor), in PCK rat livers. Extensive expression of YAP and its target genes was also detected in human ARPKD/CHF liver samples. Finally, pharmacological inhibition of YAP activity with verteporfin and short hairpin (sh) RNA-mediated knockdown of YAP expression in isolated liver CWECs significantly reduced their proliferation. These data indicate that increased YAP activity, possibly through dysregulation of the Hippo signaling pathway, is associated with hepatic cyst growth in ARPKD/CHF.

**Key words: Proliferation; Cyst; Hippo kinase; Fibrosis; Inflammation**

### INTRODUCTION

Polycystic kidney disease (PKD) is a heritable genetic disorder characterized by the formation and growth of fluid-filled cysts in ductal structures, including the kidneys and liver. Autosomal dominant PKD (ADPKD), the more common form of the disease (1 in 500 people affected), is caused by mutations in *PKD1* or *PKD2*, which code for polycystin-1 and polycystin-2, respectively<sup>1–3</sup>. Autosomal recessive PKD (ARPKD), a rare form of the disease (1 in 20,000 people affected), is caused by mutations in *PKHD1*, which encodes fibrocystin<sup>4</sup>. All three proteins are localized to the primary cilia on epithelial cells. However, it remains unclear how disruption of these ciliary proteins induces epithelial cyst formation<sup>5,6</sup>. The liver is the major extrarenal organ affected in PKD. In 60% of ADPKD and 100% of ARPKD patients, large fluid-filled cysts develop

in the liver, resulting in hepatic enlargement, inflammation, and fibrosis, which significantly contribute to the morbidity associated with PKD<sup>7–9</sup>.

Hepatic cytogenesis and associated complications are especially problematic in ARPKD. ARPKD patients develop hepatic cysts surrounded by extensive pericystic fibrosis during the perinatal period and suffer from congenital hepatic fibrosis (CHF)<sup>7–9</sup>. ARPKD/CHF patients exhibit significant portal hypertension secondary to pericystic fibrosis. Recent studies have characterized ARPKD/CHF as a major pediatric liver disorder with significant mortality<sup>5</sup>. Aside from symptom management, the only treatment option for ARPKD/CHF patients is liver and kidney transplantation.

The hepatic cysts in PKD are made up of epithelial cells that originate from dysgenesis of biliary epithelium<sup>10</sup>.

<sup>1</sup>Current Address: Department of Pediatrics, the Third Hospital of Hebei Medical University, Shijiazhuang, Hebei, P.R. China.

<sup>2</sup>Current Address: Department of Pediatric Gastroenterology, University of Colorado School of Medicine, Children's Hospital Colorado, Aurora, CO, USA.

Address correspondence to Udayan Apte, Ph.D., DABT, Department of Pharmacology, Toxicology and Therapeutics, University of Kansas Medical Center, 3901 Rainbow Boulevard, MS1018, Kansas City, KS 66160, USA. Tel: (913) 588-9247; E-mail: [uapte@kumc.edu](mailto:uapte@kumc.edu)

One of the main aspects of ARPKD/CHF pathogenesis is the aberrant proliferation of cyst wall epithelial cells (CWECs)<sup>6,11</sup>. The mechanisms responsible for CWEC proliferation remain unclear. Recent studies have shown that deregulation of the Hippo signaling pathway results in increased expression and activity of its downstream effector Yes-associated protein (YAP), which is involved in a number of fibroproliferative hepatic disorders including hepatic fibrosis, hepatocellular carcinoma, and cholangiocarcinoma<sup>12–15</sup>. When the Hippo signaling pathway is “on,” activation of LATS1/2 kinases directly phosphorylates YAP, which inhibits YAP nuclear translocation. When the Hippo signaling pathway is “off,” YAP is translocated to the nucleus and binds to different transcription factors to regulate target genes involved in cell proliferation, cell survival, and apoptosis<sup>16,17</sup>. A previous study showed increased YAP activation in kidney cyst epithelial cells from ADPKD and ARPKD patients<sup>18</sup>; however, the role of YAP in hepatic cyst development in ARPKD/CHF is not known. Our studies were undertaken to determine the role of YAP in liver CWEC proliferation with the use of human ARPKD/CHF liver tissues and animal models of ARPKD/CHF.

## MATERIALS AND METHODS

### *Animals*

Male and female polycystic kidney (PCK) rats and Sprague–Dawley (SD) rats (control strain for PCK) were purchased from Charles River and housed in an AAALAC-approved vivarium at the University of Kansas Medical Center (KUMC). *Pkhd1*<sup>LSL(-)/LSL(-)</sup> mice on a C57BL/N background were a gift from Dr. Christopher J. Ward (KUMC)<sup>19</sup>; wild-type (WT) mice on the same genetic background purchased from Charles River (Wilmington, MA) were used for controls. All animal studies were approved by the KUMC Institutional Animal Care and Use Committee (IACUC) and were performed in accordance with IACUC guidelines.

### *Tissue Harvest and Processing*

Rats ( $n = 3–4$  per time point) were euthanized under isoflurane anesthesia, and livers were harvested at postnatal days 0, 5, 10, 15, 20, 30, and 90. Livers were processed for obtaining paraffin sections and frozen sections, total cell extracts, and RNA as described before<sup>15,20</sup>. Body weights and liver weights were recorded at the time of euthanasia.

### *Histopathological Analysis*

Formalin-fixed, paraffin-embedded liver sections were used for morphological analysis and immunohistochemical staining, and frozen liver sections were used for

immunofluorescence staining. Cells were cultured on coverslips to appropriate density and fixed with 4% paraformaldehyde for immunofluorescence staining. Hematoxylin and eosin (H&E)-stained sections were used to determine the number of hepatic cysts. The source and details of primary antibodies used in these studies are as follows: proliferating cell nuclear antigen [PCNA; monoclonal antibody (mAb); clone PC10; Cell Signaling Technologies, Danvers, MA, USA], phospho-YAP (Ser127) [polyclonal antibody (pAb); Cat. No. 4911; Cell Signaling Technologies], cyclin D1 (mAb; clone 92G2; Cell Signaling Technologies), Ki-67 (pAb; Cat. No. ab-15580; Abcam, Cambridge, MA, USA), YAP (pAb; Cat. No. 4912; Cell Signaling Technologies; Cat. No. sc-101199; Santa Cruz Biotechnology, Santa Cruz, CA, USA), cytokeratin 19 (CK19; pAb; Cat. No. sc-33119; Santa Cruz Biotechnology), connective tissue growth factor (CTGF; pAb; Cat. No. sc-14939; Santa Cruz Biotechnology), and  $\beta$ -actin (mAb; clone 13E5; Cell Signaling Technologies). Secondary antibodies for immunohistochemistry and immunofluorescence were purchased from Jackson ImmunoResearch (West Grove, PA, USA). Primary antibodies were used at a concentration of 1:100 (except PCNA, which was used at a concentration of 1:5,000), and secondary antibodies were used at a concentration of 1:500. Micrographs were taken using an Olympus BX51 microscope with an Olympus DP71 camera. DP Controller software was used to acquire images at indicated magnifications (Olympus, Waltham, MA, USA).

### *RNA Isolation, cDNA Synthesis, and Real-Time PCR*

Total RNA was isolated from liver pieces and biliary trees as described previously<sup>21</sup>. Briefly, tissues (25–30 mg) were homogenized using an MP Biomedicals Fast Prep 24 bead homogenizer with lysing matrix D homogenization tubes (Solon, OH, USA). Total RNA was isolated using the Qiagen RNeasy Mini Kit (Valencia, CA, USA). Template cDNA was obtained by reverse transcription of 4  $\mu$ g of total RNA using the Retroscript kit (Life Technologies/Ambion, Grand Island, NY, USA). Real-time PCR was performed with a Bio-Rad CFX384, and the results were calculated using the  $2^{-\Delta\Delta Ct}$  method. The primers used in this study were as follows: rat *Ccnd1*, GCCCTAGCTGCCTACCGACT (forward) and ACAGGCTTG GCAATTTTAGGC (reverse); rat *Ctgf*, GCCCTAGCTGCCTACCGACT (forward) and ACAG GC TTGGCAATTTTAGGC (reverse); rat *Acta2*, AGC TCTGGTGTGTGACAATGG (forward) and GGAGCA TCATCACCAGCAAAG (reverse); rat *Ck7*, AGGAGA TCAACCGACGCAC (forward) and GTCTCGTGAAG GGTCTTGAGG (reverse); and human *CTGF*, AAAAG TGCATCCGTACTCCCA (forward) and CCGTCGGTA CATACTCCACAG (reverse).

### *ARPKD/CHF Patient Liver Tissue Samples*

Paraffin-embedded liver tissue blocks ( $n=3$ ) and frozen liver tissues ( $n=5$ ) of ARPKD/CHF patient livers were obtained from the KUMC's Liver Center Tissue Bank, PKD Biomarkers and Biomaterials Core at KUMC, the Mayo Clinic (Dr. Peter Harris), and Children's Mercy Hospital, Kansas City, MO, USA. All studies were approved by the IRB at the associated institutions.

### *CWEC Isolation*

CWECs from PCK rats were isolated as described by LaRusso and colleagues<sup>22</sup>. Briefly, biliary tree was obtained by removing hepatocytes after liver perfusion with a 37°C collagenase-containing solution. After cutting the biliary tree into small pieces with sterile scissors, the tissue was further digested in 25 ml of MEM medium (Corning, Hanover Park, IL, USA) containing 25 mM HEPES (Sigma-Aldrich, St. Louis, MO, USA), 10 mg of hyaluronidase (Sigma-Aldrich), 8 mg of collagenase P (Roche, Indianapolis, IN, USA), and 6 mg of DNase (Sigma-Aldrich) for 45 min in a 42°C water bath. The tissue pieces were gravity sedimented, washed with cold MEM, and resuspended in DMEM/F12 media (Invitrogen, Grand Island, NY, USA) supplemented with 1% penicillin–streptomycin (P/S; Invitrogen), 1% insulin–transferrin–selenium (ITS; Invitrogen),  $10^{-7}$  M dexamethasone (Sigma-Aldrich), and 5% fetal bovine serum (FBS; Sigma-Aldrich). The tissue pieces were subsequently placed in a 150-mm tissue culture dish and incubated for 2 h at 37°C, then resuspended in DMEM/F12 growth medium containing 5% FBS, 1% ITS, 4.11 µg/ml forskolin (Sigma-Aldrich), 393 ng/ml dexamethasone, 3.4 µg/ml 3,3',5-triiodo-L-thyronine (Sigma-Aldrich), 1% P/S, 25 ng/ml epidermal growth factor (Life Technologies), and 30 µg/ml bovine pituitary extract (Invitrogen), and poured into a tissue culture dish containing collagen gel. After 2–3 days of culture, cysts formed from proliferating CWECs were digested with collagenase P, trypsinized, and plated on collagen-coated plates to form cell monolayers.

### *Cell Proliferation Assay*

Cell proliferation was measured as described by Yamaguchi et al.<sup>23</sup>. Briefly, PCK CWECs were seeded in a 96-well culture plate and incubated in DMEM/F12 with 1% FBS, ITS, and P/S. After 24 h, the medium was changed to a 0.002% FBS without ITS. Cells were incubated for another 24 h before the addition of 0.1, 0.5, 2, and 5 µM verteporfin (VP; a YAP–TEAD interaction inhibitor that prevents YAP-mediated gene transcription) with or without forskolin (a cAMP agonist). After 48 h, cell proliferation was determined based on the production of formazan from the CellTiter 96 Aqueous One

Solution Cell Proliferation Assay (Promega, Madison, WI, USA). The amount of formazan is directly proportional to the number of living cells in the culture.

### *YAP Knockdown in Isolated CWECs*

YAP knockdown experiments were conducted in primary liver CWECs isolated from PCK rats. Cells were transfected with either control short hairpin RNA (shRNA) (sc-108080; Santa Cruz Biotechnology) or YAP shRNA (sc-38638-V; Santa Cruz Biotechnology) for 24 h. Cell proliferation rate was assessed by cell proliferation assay described above. Interference efficiency was detected by Western blotting. The ratio of YAP/β-actin was quantified with three independent Western blot results using the ImageJ software.

### *Statistics*

All data are represented as the mean ± standard error of the mean. Student's *t*-test was used to calculate differences between two groups. One-way ANOVA or two-way ANOVA was used depending on comparisons performed. Tukey's adjustment for multiple comparisons was used where appropriate. In each case, a value of  $p < 0.05$  was considered statistically different.

## RESULTS

### *Extensive Proliferation in PCK Rat Livers*

Using H&E-stained liver sections from PCK and SD rats, we evaluated liver histology from postnatal day (PND) 0 to PND 90. Hematopoietic cells (clusters of small cells with basophilic nuclei) were evident in the livers of SD rats on PND 0 and PND 5 but were absent at PND 10 (Fig. 1A). This observation is consistent with the hematopoietic nature of the perinatal liver<sup>24</sup>. The portal vein, hepatic artery, and bile ducts (the portal triad) were readily identifiable in livers from SD rats from PND 10 onward and did not change in appearance through PND 90 (Fig. 1A). Similar to SD rats, PCK rat livers contained hematopoietic cells at PND 0 and PND 5 but not PND 10 onward (Fig. 1A). Bile ducts were dilated in livers from PCK rats from PND 0 onward, and the number of cysts developing from dilated bile ducts increased throughout the time course, disrupting normal portal triad histological structure (Fig. 1A). To determine if there was elevated proliferation of CWECs, we stained liver sections from PCK and SD rats with antibodies recognizing PCNA (Fig. 1B) and cyclin D1 (Fig. 1C), markers for cell proliferation. Overall, we found more PCNA<sup>+</sup> and cyclin D1<sup>+</sup> cells in the liver of PCK rats compared to that in SD rats, and the PCNA<sup>+</sup>/cyclin D1<sup>+</sup> cells were not limited to CWECs. In order to gain a better insight into CWEC proliferation at the

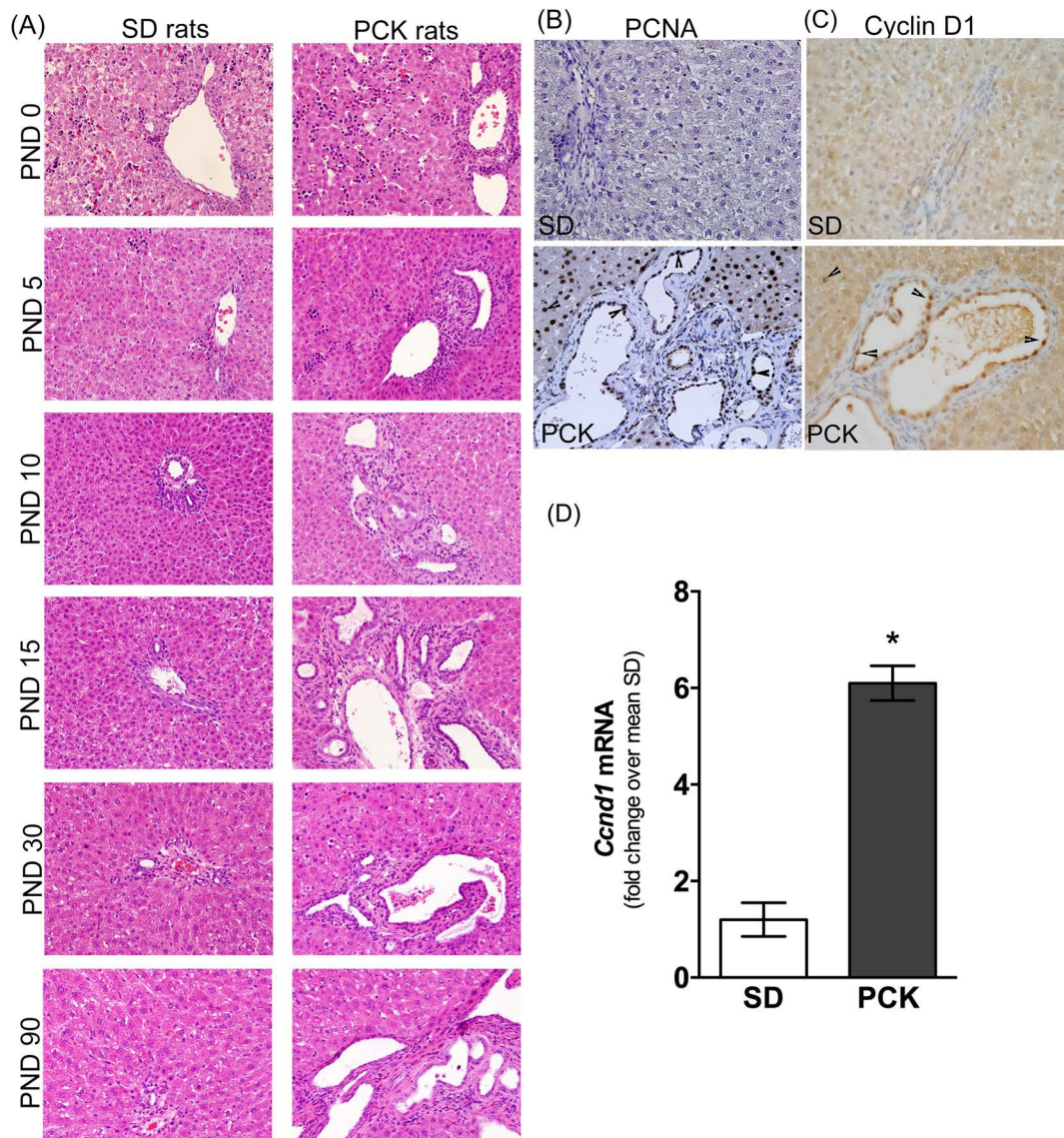


**Figure 1.** Cyst growth and proliferation in polycystic kidney (PCK) rat livers. (A) Representative photomicrographs of hematoxylin and eosin (H&E)-stained livers from Sprague–Dawley (SD) and PCK rats from postnatal day (PND) 0 to PND 90 (3 months). Immunostaining for proliferating cell nuclear antigen (PCNA) (B) and cyclin D1 (C) in SD and PCK rat liver sections. Images were taken at 400 $\times$  magnification. Arrowheads indicate PCNA<sup>+</sup> cells (B) or cyclin D1<sup>+</sup> cells (C). (D) *Ccnd1* transcript level in biliary trees from 6-month-old SD and PCK rats.  $n=4$  rats per group. \* $p<0.05$  between genotypes.

mRNA level, we measured *Ccnd1* transcripts in biliary trees isolated from 6-month-old SD and PCK rats. Consistent with immunohistochemistry staining, *Ccnd1* mRNA was significantly upregulated in PCK rat biliary trees (Fig. 1D).

#### Increased YAP Expression in CWECs From PCK Rats and *Pkhd1*<sup>LSL(-)/LSL(-)</sup> Mice

Moderate YAP expression was observed in cholangiocytes from SD rat livers (Fig. 2A). Higher YAP expression

with nuclear localization was observed in the CWECs from PCK rats (Fig. 2A and B). In the canonical Hippo signaling pathway, phosphorylated YAP is sequestered in the cytoplasm and targeted for degradation<sup>25</sup>. Thus, the ratio of YAP to phospho-YAP is a surrogate marker of YAP activity. Immunohistochemistry for phospho-YAP revealed only moderate cytoplasmic staining in CWECs from PCK rat livers (Fig. 2B). To further investigate the expression of YAP in another model of ARPKD/CHF, we performed YAP staining on liver samples from WT mice

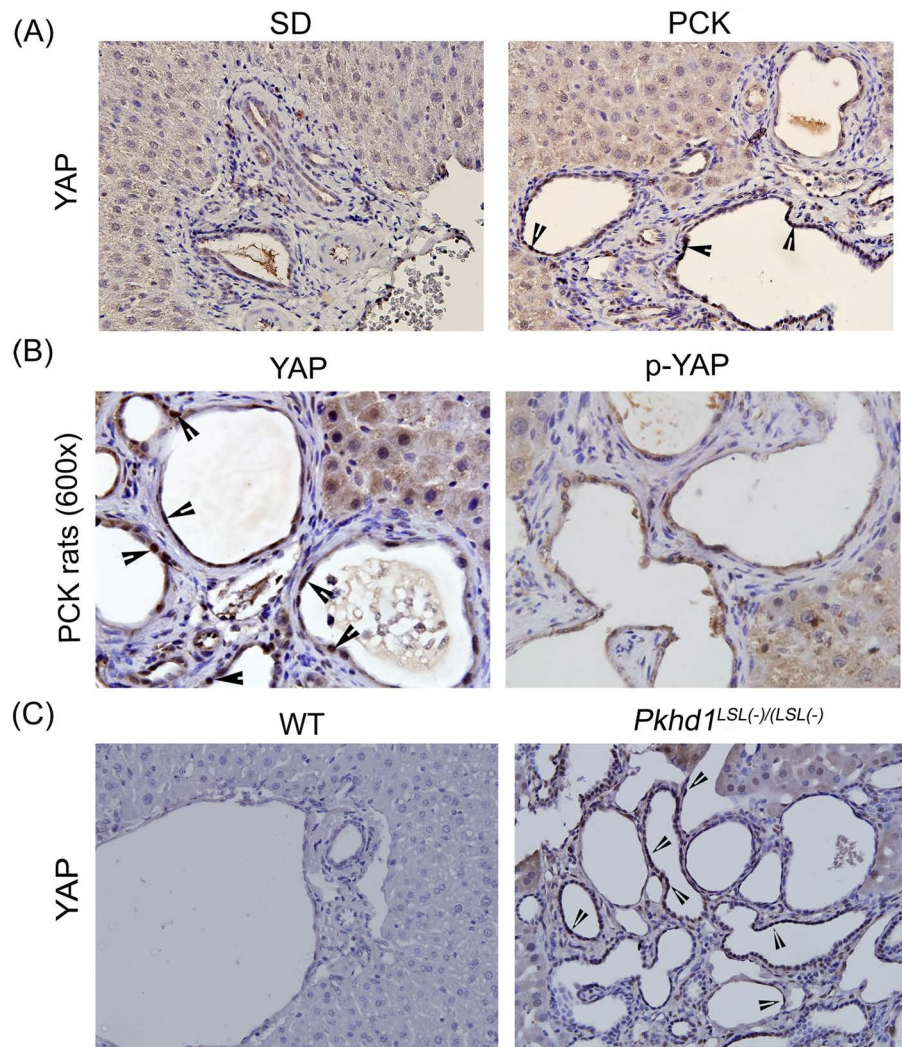


**Figure 2.** Increased Yes-associated protein (YAP) activation in PCK rat livers. (A) Representative photomicrographs (400 $\times$ ) of YAP immunohistochemistry in SD and PCK rat livers. (B) Representative photomicrographs (600 $\times$ ) of YAP and phospho-YAP immunohistochemistry in PCK rat livers. Arrowheads point to cyst wall epithelial cells (CWEC) positive for YAP. (C) Representative photomicrographs (400 $\times$ ) of YAP immunohistochemistry in wild-type (WT) and *Pkhd1*<sup>LSL(-)/LSL(-)</sup> mice.

and *Pkhd1*<sup>LSL(-)/LSL(-)</sup> mice. Similarly, liver samples from *Pkhd1*<sup>LSL(-)/LSL(-)</sup> mice exhibited higher YAP nuclear staining in comparison to the liver samples from WT mice (Fig. 2C).

#### *YAP Is Actively Expressed in Proliferating PCK Rat Liver CWECs*

To confirm the association between YAP and CWECs, we performed coimmunofluorescence (co-IF) staining for CK19, a biliary epithelial cell marker, and YAP in PCK rat livers. Our co-IF studies showed YAP and CK19 colocalization in the biliary epithelium from SD rats (Fig. 3A); more colocalization of YAP and CK19 was observed in CWECs from PCK rat livers (Fig. 3B).

These data suggest a strong association between YAP and CWECs in PCK rats. To test the role of YAP in CWEC proliferation, we performed co-IF to determine if YAP colocalizes with Ki-67 (a cell proliferation marker) in CWECs. As we expected, colocalization occurs only in the PCK and not in the SD rats (Fig. 4).

#### *CTGF Is Increased in Hepatic Cysts in PCK Rats*

YAP regulates the expression of connective tissue growth factor (*Ctgf*), encoding for a matricellular protein of the CNN family<sup>26-30</sup>. Real-time PCR analysis showed that hepatic *Ctgf* mRNA was greater in livers from PCK rats than in SD rats beginning at PND 10 (Fig. 5A). *Ctgf* transcript levels peaked at PND 20 and PND 30 in PCK

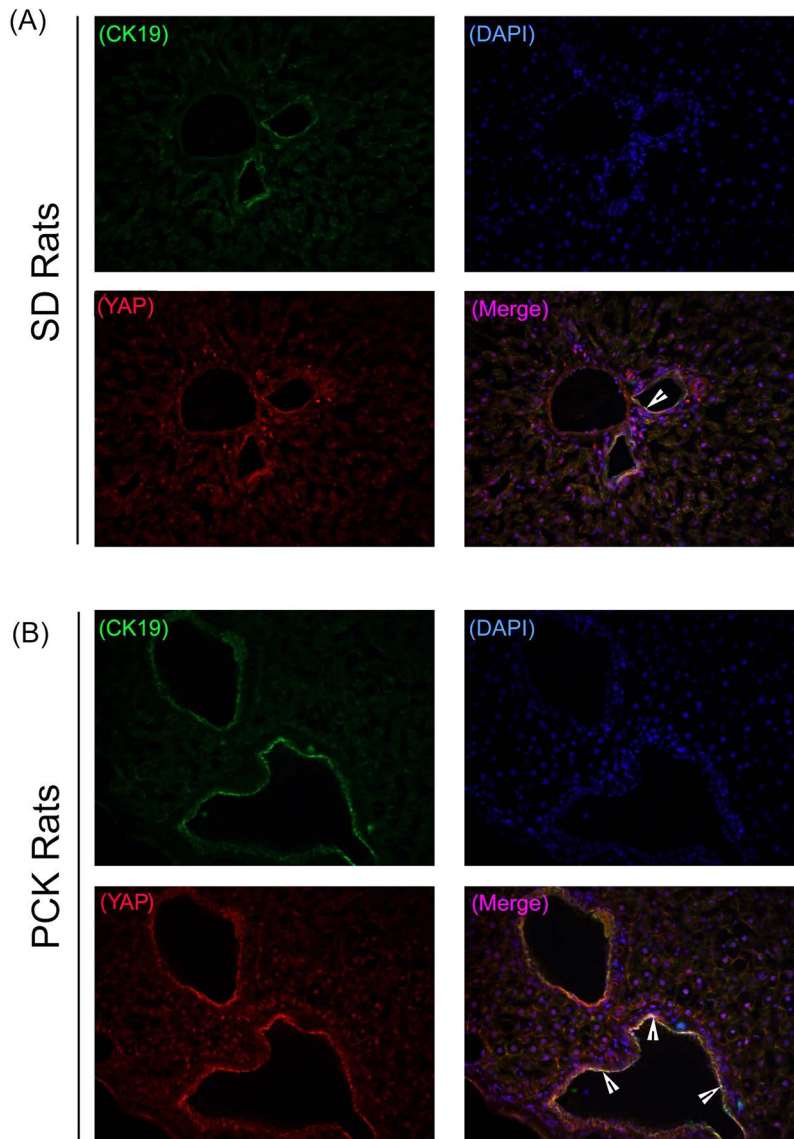


**Figure 3.** YAP and cytokeratin 19 (CK19) colocalization in CWECS. Representative photomicrographs of immunofluorescence staining of YAP (red), CK19 (green), and 4',6-diamidino-2-phenylindole (DAPI) (blue) on frozen liver sections from SD rats (A) and PCK rats (B). Images were taken at 400 $\times$ . Arrowheads point to colocalization of YAP and CK19.

rats and decreased substantially thereafter (Fig. 5A). However, *Ctgf* mRNA remained sixfold higher in the PCK rat livers compared to the SD rat livers at 90 days after birth (Fig. 5B). To determine *Ctgf* expression level in the absence of hepatocytes, we measured its expression in biliary trees isolated from 6-month-old SD rats and PCK rats (Fig. 5C). We found that the *Ctgf* expression was significantly higher in PCK rat biliary trees compared to that in SD rats. Immunohistochemical analysis revealed extensive CTGF staining in CWECS from PCK rats compared to SD rats (Fig. 5D). Interestingly, CTGF protein was also observed in cells within the pericystic fibrotic tissue and hepatocytes (Fig. 5D). Taken together,

these data suggest that increased YAP content in livers from PCK rats drives the expression of YAP target genes associated with ARPKD/CHF disease progression in PCK rats.

#### *Increased YAP, PCNA, and CTGF in Hepatic Cysts in ARPKD/CHF Patient Samples*

To determine YAP expression pattern in hepatic cysts in human ARPKD/CHF, we performed immunohistochemistry on paraffin-embedded liver sections from two ARPKD/CHF patients. Serial sections stained with H&E (Fig. 6A), or with antibodies recognizing PCNA (Fig. 6B) or YAP (Fig. 6C and enlarged in Fig. 6D), revealed

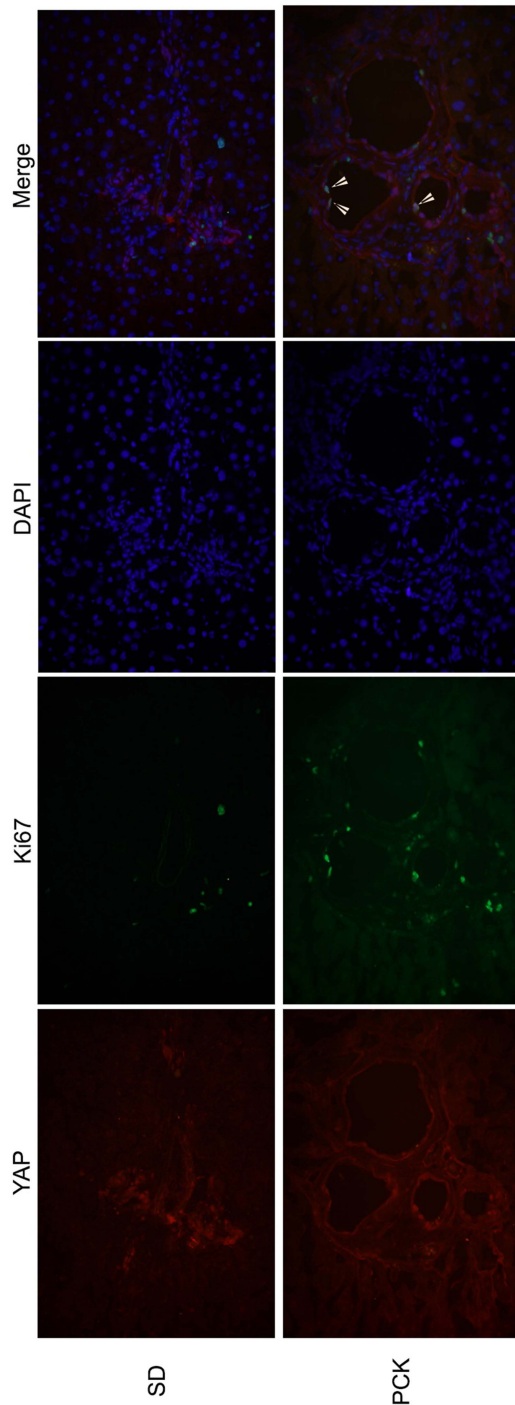


**Figure 4.** YAP/Ki-67 colocalization is increased in PCK CWECs. Representative images of immunofluorescence staining of YAP (red), Ki-67 (green), and DAPI (blue) on liver sections from SD and PCK rats are shown at 400 $\times$  magnification. Arrowheads point to colocalization of YAP, Ki-67, and DAPI.

extensive YAP expression with nuclear localization in CWECs, which also stained positive for PCNA.

We also evaluated CTGF content in patient-derived liver samples. We evaluated hepatic *CTGF* transcript levels using real-time PCR in three normal human liver samples and three liver samples from patients with ARPKD/CHF. Although, there was variation in relative *CTGF* expression (Fig. 6E), there was a trend toward increased *CTGF* expression in this limited number of samples. An immunohistochemical approach revealed substantial CTGF positivity in CWECs as well as in cells found in the pericystic fibrotic areas (Fig. 6F and enlarged in Fig. 6G). Collectively, these data suggest that, similar to findings in the PCK rat, nuclear YAP content is a prominent feature of proliferating CWECs found in ARPKD/CHF patients and is associated with hepatic CTGF content accumulation.

#### *The YAP–TEAD Binding Disruptor Verteporfin (VP) Inhibits CWEC Proliferation*

YAP is not able to bind DNA directly and therefore requires interaction with bona fide transcription factors to regulate gene transcription. TEAD (TEA domain family member) is a transcription factor and one of the best-characterized binding partners of YAP<sup>31</sup>. VP is a chemical inhibitor of the YAP–TEAD interaction and prevents YAP-mediated gene regulation<sup>32</sup>. To explore the role of YAP in CWEC proliferation, we examined the ability of VP to inhibit the function of YAP in CWEC proliferation in vitro. We first isolated CWECs from PCK rats and characterized them by light microscopy, co-IF staining, and real-time PCR. After isolation, CWECs were cultured, as a monolayer, onto collagen gel-coated plates. CWECs formed colonies of cells with a cobblestone pattern characteristic of primary epithelial cells in culture (Fig. 7A). To confirm that the isolated CWECs still maintained the nuclear staining of YAP, we performed co-IF for YAP and CK19 on cultured CWECs. Consistent with co-IF staining in vivo, the PCK CWECs stained positive for both YAP and CK19, confirming that these primary cells were derived from cholangiocytes, and they maintain the YAP<sup>+</sup> feature in vitro (Fig. 7B). This was further confirmed by real-time PCR analysis for an additional cholangiocyte marker, *Ck7*. As shown in Figure 7C, CWECs were enriched for *Ck7* transcripts relative to biliary tree isolated from SD and PCK rats or relative to whole liver from SD rats. To exclude the possibility of myofibroblast contamination in our CWEC cultures, we quantified *Acta2* transcripts ( $\alpha$  smooth muscle actin gene) in CWEC cultures by real-time PCR. CWECs did not express *Acta2*, whereas *Acta2* was found in biliary tree isolated from SD and PCK rats (Fig. 7D) due to fibroblasts found in the connective tissue surrounding the biliary tree. Interestingly, we found that the *Acta2* level was significantly lower in biliary trees from PCK rats. It

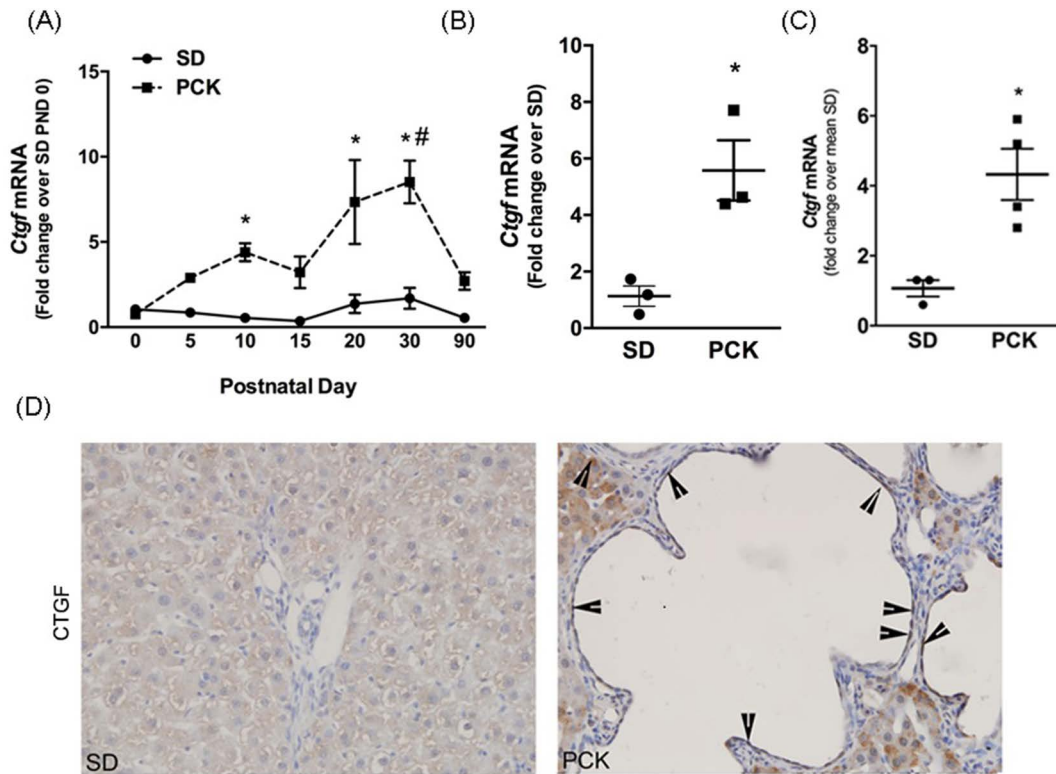


**Figure 5.** Connective tissue growth factor (CTGF) expression in livers from PCK rats. (A) Real-time PCR was used to quantify hepatic *Ctgf* transcripts in livers from SD and PCK rats from PND 0 to PND 90.  $n=3-4$  rats per time point. (B) *Ctgf* transcript content in SD and PCK rats on PND 90.  $n=3$  rats in each group. (A, B) Circles indicate SD data, and squares indicate PCK data. (C) *Ctgf* transcript content in biliary trees from 6-month-old SD and PCK rats.  $n=4$  rats in each group. (D) Representative CTGF immunohistochemistry from PCK rats at PND 90. Images were taken at 400 $\times$  magnification. Arrowheads indicate CTGF<sup>+</sup> cells. \* $p<0.05$  between genotypes at the given time point; # $p<0.05$  compared to PND 90.

is possibly due to the increased proportion of CWECs in PCK rats compared to the normal cholangiocytes in the SD biliary tree. *Acta2* was not detectable in livers from SD rats (Fig. 7D).

Next, to determine the role of YAP in aberrant cell proliferation in PCK rats, we treated CWECs with various concentrations (0.1, 0.5, 2, and 5  $\mu\text{M}$ ) of VP alone or in combination with forskolin. Forskolin is a cAMP agonist that stimulates renal cystic epithelial cell proliferation in ADPKD through activation of the B-Raf/MEK/ERK pathway<sup>33,34</sup>. VP treatment alone significantly reduced CWEC proliferation at a dose of 0.1  $\mu\text{M}$  compared to the DMSO control (Fig. 8A). Furthermore, VP at higher doses exhibited a greater degree of inhibition on CWEC proliferation. Forskolin treatment caused a significant increase in CWEC proliferation, consistent with previous results<sup>35</sup>. Treatment with VP blocked forskolin-mediated CWEC proliferation (Fig. 8A). These data suggest that the inhibitory effect of VP on CWEC proliferation may occur downstream of a cAMP-mediated pathway. The inhibitory effect of VP on YAP-mediated gene expression was confirmed by a significant reduction of *Birc5*

(survivin gene) expression (Fig. 8B). The ability of VP to inhibit CWEC proliferation in our model is consistent with the observation that VP can block the proliferation in cholangiocyte and cholangiocarcinoma cell lines<sup>36</sup>.

#### YAP Knockdown Decreases CWEC Proliferation

As a second approach to perturb YAP-mediated gene expression, we performed a YAP knockdown experiment in isolated CWECs using shRNA. Western blot analysis indicated a modest but significant decrease in total YAP protein in cells treated with YAP shRNA (Fig. 8C and D). Further, a cell proliferation assay indicated a significant decrease in cell proliferation after YAP shRNA treatment for 24 h (Fig. 8E). Taken together, these data support the hypothesis that aberrant proliferation of the CWECs is mediated, at least in part, by YAP.

## DISCUSSION

ARPKD/CHF is a rare but devastating and progressive genetic disease that is especially debilitating in pediatric patients<sup>9,37</sup>. Hepatic complications due to rapidly



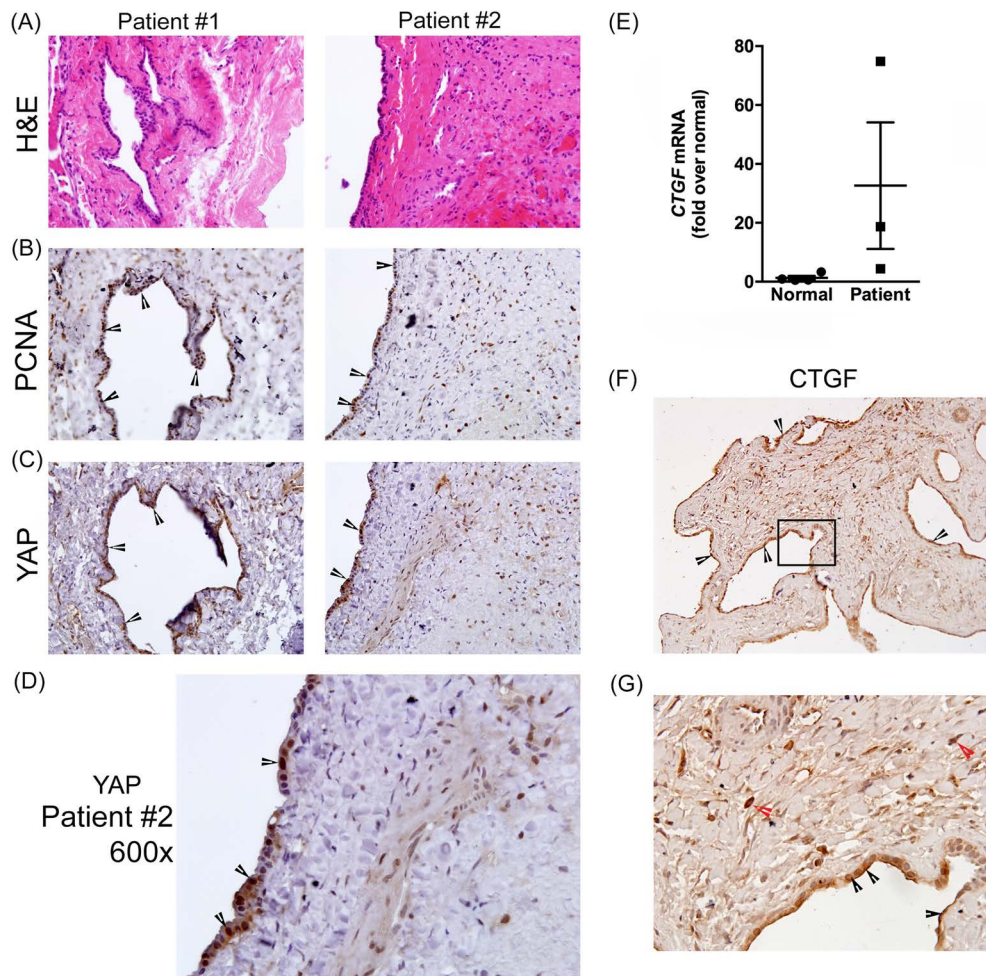


**Figure 6.** Characterization of YAP expression, cell proliferation, and CTGF in human Autosomal recessive PCK (ARPKD)/congenital hepatic fibrosis (CHF) livers. Representative photomicrographs of H&E-stained liver sections (A) showing hepatic cysts and surrounding pericystic tissue, and PCNA (B) and YAP (C) immunostaining in two different ARPKD/CHF patients. (D) Enlarged image (600 $\times$ ) of YAP immunostaining from patient #2. (E) Real-time PCR was used to measure hepatic *CTGF* transcripts in three patients. (F) CTGF immunostaining in one ARPKD/CHF patient. The black box outlines the area enlarged (G). Black arrowheads point to CTGF<sup>+</sup> CWECs, and red arrowheads point to the CTGF<sup>+</sup> cells in pericystic fibrotic area.

developing cysts, accompanied by pericystic fibrosis, inflammation, and subsequent portal hypertension, lead to significant morbidity and high perinatal mortality<sup>9</sup>. Thirty to 40% of patients with this disease die in the perinatal period<sup>38</sup>. Patients that survive the perinatal period require intensive treatment that can include a simultaneous liver and kidney transplant. Unfortunately, the mechanisms of hepatic cyst development remain poorly understood, which has hindered finding alternative treatment strategies. Although we previously hypothesized that a central mechanism regulating ARPKD/CHF is a “pathogenic triumvirate” consisting of fibrogenesis, CWEC proliferation, and pericystic inflammation<sup>39</sup>, no specific signaling pathway has been implicated to date in all three processes. We propose that one pathway that could regulate all three pathogenic processes is the Hippo signaling pathway.

For example, previous studies suggest that YAP and TAZ (a related transcriptional coactivator) are key activators of fibroblasts, and they sustain fibrosis by activating fibroblasts<sup>40</sup>. As an oncoprotein, YAP activation is found in several human cancers<sup>41–44</sup>, and it plays a key role in the Hippo pathway to control cell proliferation in response to cell contact<sup>41</sup>. Finally, YAP activation promotes endothelial cell proliferation and inflammatory response in atherosclerosis<sup>45</sup>. Therefore, it is logical to predict that the Hippo signaling pathway could be the central pathway regulating each member of the pathogenic triumvirate in ARPKD/CHF.

A major component of ARPKD/CHF, apart from progressive fibrosis and inflammation, is the rapid growth of cysts due to aberrant cell proliferation and fluid secretion. Multiple mechanisms are implicated in the regulation of

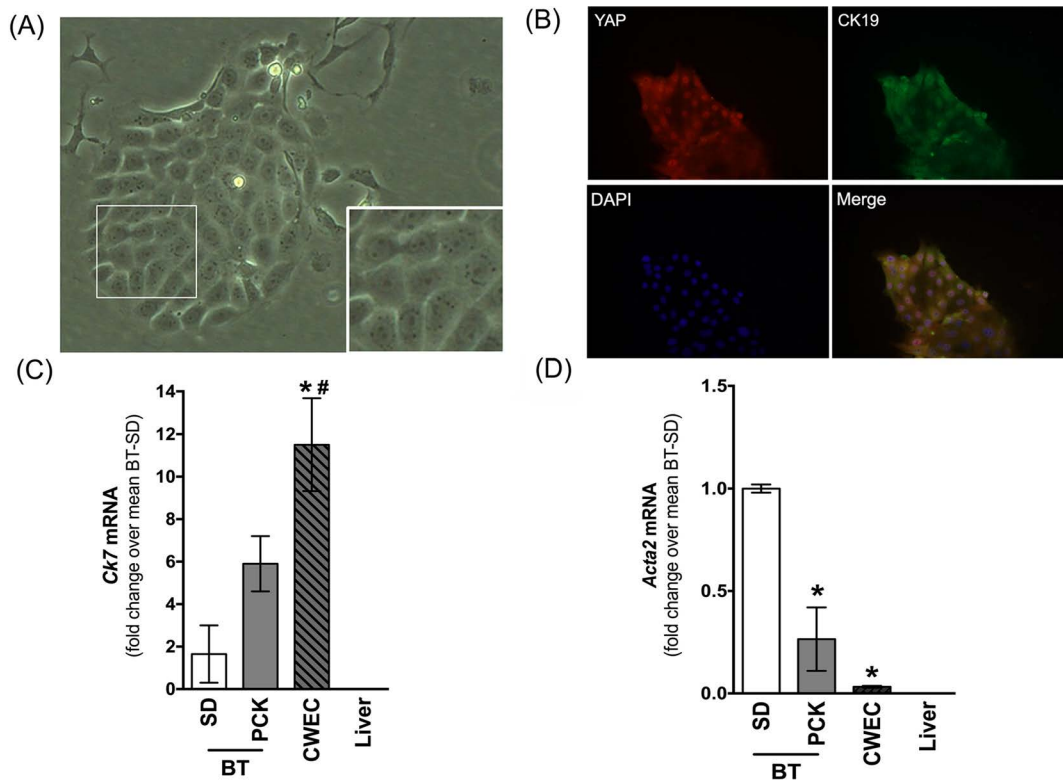


**Figure 7.** Characterization of CWECs isolated from PCK rats. (A) Representative phase-contrast micrograph of CWEC growing on collagen gel-coated plates as a monolayer (400 $\times$ ). The area demarcated by the white box in the image is enlarged in the inset in the bottom right of the same image. (B) Representative immunofluorescence image (400 $\times$ ) of CK19 staining in isolated CWECs. Real-time PCR analysis of *Ck7* (cytokeratin 7, a cholangiocyte marker, C) and *Acta2* ( $\alpha$ SMA, a fibroblast marker, D) from SD rat biliary tree (BT), PCK rat BT, PCK CWEC, and SD liver. Liver=whole liver from SD rats. \* $p$ <0.05 versus SD BT; # $p$ <0.05 versus liver.

CWEC proliferation including calcium and cAMP signaling, the B-Raf/MEK/ERK pathway, VEGF, Cdc25A, HDAC6, and Wnt signaling due to LRP5 mutations<sup>46–52</sup>. Recent studies have highlighted the role of YAP in the regulation of normal and abnormal cell proliferation during postnatal liver growth and cancer pathogenesis<sup>13–14,53–56</sup>. Interestingly, increased YAP activation is also observed in kidney cyst development in ADPKD<sup>18</sup>. Importantly, that study demonstrated increases in renal YAP target genes, *Birc3*, *Ctgf*, *InhibA*, and *Fjx1*, a planar cell polarity gene, in *Pkd1*-deleted mice and in renal tissues from ADPKD patients<sup>18</sup>. Our results are consistent with these studies. However, our study is the first to demonstrate that hepatic CWECs have significant YAP overexpression and activation as demonstrated by increased nuclear YAP localization and increased expression of YAP target genes in animals and patients with ARPKD/CHF. Therefore, our data suggest that hepatic cystogenesis is associated with deregulation of the Hippo signaling pathway.

In this study, we used PCK rats, a variant of the SD rat strain, which harbors a single splicing mutation (IVS35-2A $\Delta$ T) in the rat ortholog of human *PKHD1*, the gene found mutated in human ARPKD/CHF; the PCK rat

develops renal and hepatic pathology similar to human ARPKD/CHF<sup>57–59</sup>. We found increased levels of cyclin D1 and PCNA expression in the CWECs, consistent with increased levels of cell proliferation. In addition to CWECs, cyclin D1 and PCNA<sup>+</sup> cells were increased in the periportal area of PCK rat livers, suggesting that other secreted factors, possibly CTGF, promote the proliferation of hepatocytes or other interstitial cells. The mechanisms of hepatocyte proliferation and their relation to cyst enlargement are unknown. Previous studies indicated that extensive shear stress in the liver may induce proliferative changes<sup>60</sup>, and it is possible that mechanical stress induced by enlarging cysts may stimulate similar changes in hepatocytes. Interestingly, a precedent for YAP/TAZ as mechanosensors capable of detecting and responding to the extracellular environment has already been established, suggesting that cystogenesis and cyst growth may regulate the Hippo signaling pathway in ARPKD/CHF<sup>61</sup>. For example, interactions between primary cilia, polycystin (defective in ADPKD), and YAP/TAZ likely occur and function as a mechanosensing system in response to alterations in extracellular matrix stiffness<sup>62</sup>. Therefore, it is possible that fibrocystin deficiency in ARPKD/CHF

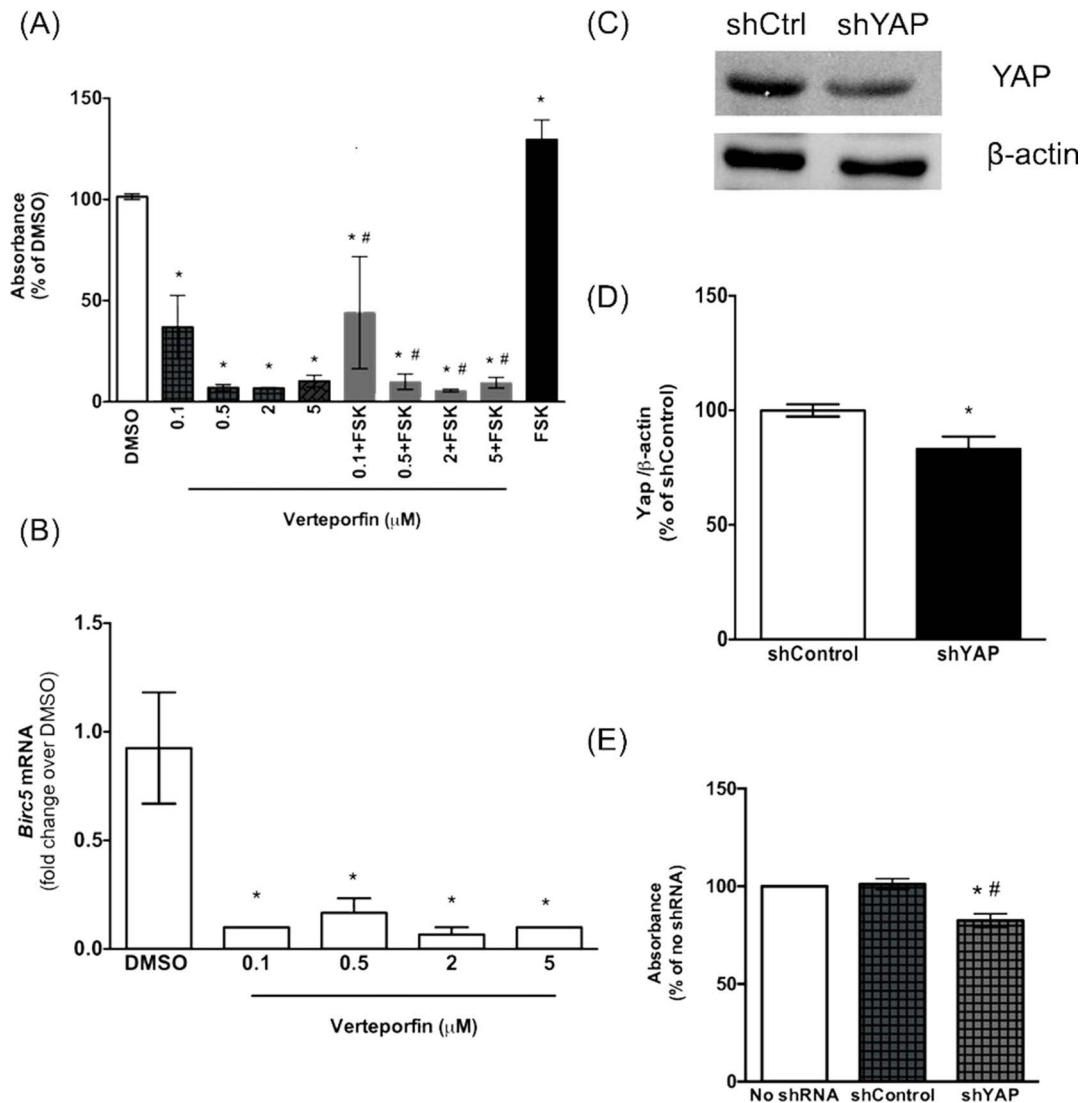


**Figure 8.** CWEC proliferation is reduced after inhibition of YAP activity with verteporfin (VP) and YAP knockdown in vitro. (A) Effects of different concentrations of VP on cell proliferation. CWECs were treated with the indicated VP concentrations with or without forskolin (FSK). DMSO was used as control. (B) Real-time PCR analysis of *Birc5* transcripts after VP treatment. \*Significant decrease ( $p < 0.05$ ) relative to the DMSO; #significant decrease ( $p < 0.05$ ) relative to FSK. (C, D) Western blotting analysis of total YAP protein after YAP short hairpin (shRNA)-mediated knockdown. The YAP band intensity was normalized to  $\beta$ -actin. (E) Effect of YAP knockdown on CWEC proliferation. Each experiment was repeated three times (CWECs from three separate biliary trees from three separate rats isolated on 3 separate days). The error bars represent the standard error of mean. \*Significant decrease ( $p < 0.05$ ) relative to the no shRNA treatment group; #significant decrease ( $p < 0.05$ ) relative to control shRNA.

leads to YAP/TAZ activation by a mechanism involving defective primary cilia.

Our data revealed that CWECs have YAP activation in both PCK rats and in ARPKD/CHF patient livers. CWECs in rat and human livers show YAP nuclear localization and increased expression of the YAP target gene *Ctgf*. The increase in *Ctgf* was particularly interesting because of its involvement in ECM synthesis and fibrosis<sup>26,28</sup>. *Ctgf* expression was also increased in pericyclic cells, suggesting roles for YAP and CTGF not only in CWEC

proliferation but also in fibrosis associated with ARPKD/CHF. Interestingly, cross-talk between cholangiocytes and myofibroblasts has been suggested by Locatelli et al.<sup>63</sup>. By secreting chemokines (CXCL1, CXCL10, and CXCL12), cholangiocytes recruit macrophages, which leads to further macrophage-mediated TGF $\beta$ 1 activation, resulting in hepatic stellate cell activation and collagen accumulation<sup>63</sup>.

A previous study suggests that VP is an effective inhibitor of the YAP-TEAD interaction required for

YAP-mediated gene expression and exhibits few side effects<sup>32</sup>. This novel VP function is independent of its current clinical application as a photosensitizer in vascular ablation procedures for the treatment of some ocular diseases, including age-related macular degeneration<sup>64</sup>. VP-mediated blockade of the YAP–TEAD interaction does not require photoactivation as it does for its use in age-related macular degeneration yet inhibits YAP-induced liver overgrowth in vivo and in vitro<sup>32</sup>. To test the feasibility of targeting YAP-induced CWEC proliferation as a selective means of inhibiting cyst growth in liver, we inhibited YAP-regulated target gene expression with VP in vitro. We demonstrate here that VP effectively decreased CWEC proliferation in the presence and absence of forskolin. Our data indicate that the proproliferative effect of YAP is possibly functioned through the cAMP-mediated pathway. The exact molecular mechanisms remain unknown, and future work is needed to elucidate both the molecular mechanisms of YAP action and VP's efficacy in animal models of ARPKD/CHF.

In summary, our data suggest that YAP is an important contributing factor for the progression of ARPKD/CHF by promoting the proliferation of CWECs. Our study is consistent with what is currently known regarding YAP in renal cyst growth in ADPKD<sup>18</sup>. These data have identified a new potential therapeutic target (YAP) and pharmacologic strategy (VP) to reduce disease progression in the liver, and possibly the kidneys, of individuals with PKD.

**ACKNOWLEDGMENTS:** *These studies were supported by the National Institutes of Health (NIH): P20 RR021940, R01 DK098414, and AASLD/ALF Liver Scholar Award (to Udayan Apte) and P20 RR021940, P20 GM103549, P20 GM103418, and P30 DK074038 (to Michele T. Pritchard). Human samples were obtained with the assistance of the PKD Biomarkers and Biomaterials Core (Darren P. Wallace) in the Kansas PKD Research and Translational Core Center [NIH P30 DK106912 (James P. Calvet)]. The authors would like to thank the following individuals: Benjamin Roberts (KUMC Liver Center) and Dr. Peter Harris (Mayo Clinic) for the ARPKD/CHF patient samples.*

## REFERENCES

1. The European Polycystic Kidney Disease Consortium. The polycystic kidney-disease-1 gene encodes a 14 kb transcript and lies within a duplicated region on chromosome-16. *Cell* 1994;77(6):881–94. [Erratum: *Cell* 1994;81(7):i]
2. Burn TC, Connors TD, Dackowski WR, Petry LR, van Raay TJ, Millholland JM, Venet M, Miller G, Hakim RM, Landes GM, Kilnger KW, Qian F, Onuchic LF, Watnick T, Germino GG, Doggett NA. Analysis of the genomic sequence for the autosomal dominant polycystic kidney disease (PKD1) gene predicts the presence of a leucine-rich repeat. *The AMERICAN PKD1 Consortium (APKD1 Consortium). Human Molecular Genetics* 1995;4(4):575–582.
3. Mochizuki T, Wu GQ, Hayashi T, Xenophontos SL, Veldhuisen B, Saris JJ, Reynolds DM, Cai YQ, Gabow PA, Pierides A, Kimberling WJ, Breuning MH, Deltas CC, Peters DJM, Somlo S. PKD2, a gene for polycystic kidney disease that encodes an integral membrane protein. *Science* 1996;272(5266):1339–1342.
4. Igarashi P, Somlo S. Genetics and pathogenesis of polycystic kidney disease. *J Am Soc Nephrol.* 2002;13(9):2384–98.
5. Turkbey B, Ocak I, Daryanani K, Font-Montgomery E, Lukose L, Bryant J, Tuchman M, Mohan P, Heller T, Gahl WA, Choyke PL, Gunay-Aygun M. Autosomal recessive polycystic kidney disease and congenital hepatic fibrosis (ARPKD/CHF). *Pediatric Radiology* 2009;39(2):100–111.
6. Lazaridis KN, LaRusso NF. The cholangiopathies. *Mayo Clin Proc* 2015.
7. Everson GT, Helmke SM, Doctor B. Advances in management of polycystic liver disease. *Expert Rev Gastroenterol Hepatol.* 2008;2(4):563–76.
8. Everson GT, Taylor MR, Doctor RB. Polycystic disease of the liver. *Hepatology* 2004;40(4):774–82.
9. Wen J. Congenital hepatic fibrosis in autosomal recessive polycystic kidney disease. *Clin Transl Sci.* 2011;4(6):460–5.
10. Masyuk T, Masyuk A, LaRusso N. Cholangiociliopathies: genetics, molecular mechanisms and potential therapies. *Curr Opin Gastroenterol.* 2009;25(3):265–71.
11. Masyuk T, LaRusso N. Polycystic liver disease: New insights into disease pathogenesis. *Hepatology* 2006;43(5):906–8.
12. Camargo FD, Gokhale S, Johnnidis JB, Fu D, Bell GW, Jaenisch R, Brummelkamp TR. YAP1 increases organ size and expands undifferentiated progenitor cells. *Curr Biol.* 2007;17(23):2054–60.
13. Li H, Wolfe A, Septer S, Edwards G, Zhong X, Abdulkarim AB, Ranganathan S, Apte U. Deregulation of Hippo kinase signalling in human hepatic malignancies. *Liver Int.* 2012;32(1):38–47.
14. Pan D. The hippo signaling pathway in development and cancer. *Dev Cell* 2010;19(4):491–505.
15. Septer S, Edwards G, Gunewardena S, Wolfe A, Li H, Daniel J, Apte U. Yes-associated protein is involved in proliferation and differentiation during postnatal liver development. *Am J Physiol Gastrointest Liver Physiol.* 2012;302(5):G493–503.
16. Yu FX, Zhao B, Guan KL. Hippo pathway in organ size control, tissue homeostasis, and cancer. *Cell* 2015;163(4):811–28.
17. Di Cara F, Maile TM, Parsons BD, Magico A, Basu S, Tapon N, King-Jones K. The Hippo pathway promotes cell survival in response to chemical stress. *Cell Death Differ.* 2015;22(9):1526–39.
18. Happe H, van der Wal AM, Leonhard WN, Kunnen SJ, Breuning MH, de Heer E, Peters DJ. Altered Hippo signalling in polycystic kidney disease. *J Pathol.* 2011;224(1):133–42.
19. Bakeberg JL, Tammachote R, Woollard JR, Hogan MC, Tuan HF, Li M, van Deursen JM, Wu Y, Huang BQ, Torres VE, Harris PC, Ward CJ. Epitope-tagged Pkhd1 tracks the processing, secretion, and localization of fibrocystin. *J Am Soc Nephrol.* 2011;22(12):2266–77.
20. Walesky C, Edwards G, Borude P, Gunewardena S, O'Neil M, Yoo B, Apte U. Hepatocyte nuclear factor 4 alpha deletion promotes diethylnitrosamine-induced hepatocellular carcinoma in rodents. *Hepatology* 2013;57(6):2480–90.
21. Deshpande KT, Liu S, McCracken JM, Jiang L, Gaw TE, Kaydo LN, Richard ZC, O'Neil MF, Pritchard MT.

- Moderate (2%, v/v) ethanol feeding alters hepatic wound healing after acute carbon tetrachloride exposure in mice. *Biomolecules* 2016;6(1).
22. Muff MA, Masyuk TV, Stroope AJ, Huang BQ, Splinter PL, Lee SO, LaRusso NF. Development and characterization of a cholangiocyte cell line from the PCK rat, an animal model of autosomal recessive polycystic kidney disease. *Lab Invest.* 2006;86(9):940–50.
  23. Yamaguchi T, Hempson SJ, Reif GA, Hedge AM, Wallace DP. Calcium restores a normal proliferation phenotype in human polycystic kidney disease epithelial cells. *J Am Soc Nephrol.* 2006;17(1):178–87.
  24. Payushina OV. Hematopoietic microenvironment in the fetal liver: Roles of different cell populations. *ISRN Cell Biol.* 2012;2012:7.
  25. Hao Y, Chun A, Cheung K, Rashidi B, Yang X. Tumor suppressor LATS1 is a negative regulator of oncogene YAP. *J Biol Chem.* 2008;283(9):5496–509.
  26. Gressner OA, Gressner AM. Connective tissue growth factor: A fibrogenic master switch in fibrotic liver diseases. *Liver Int.* 2008;28(8):1065–79.
  27. Pi L, Ding X, Jorgensen M, Pan JJ, Oh SH, Pintilie D, Brown A, Song WY, Petersen BE. Connective tissue growth factor with a novel fibronectin binding site promotes cell adhesion and migration during rat oval cell activation. *Hepatology* 2008;47(3):996–1004.
  28. Pi L, Robinson PM, Jorgensen M, Oh SH, Brown AR, Weinreb PH, Trinh TL, Yianni P, Liu C, Leask A, Violette SM, Scott EW, Schultz GS, Petersen BE. Connective tissue growth factor and integrin  $\alpha$ v $\beta$ 6: A new pair of regulators critical for ductular reaction and biliary fibrosis in mice. *Hepatology* 2015;61(2):678–91.
  29. Rachfal AW, Brigstock DR. Connective tissue growth factor (CTGF/CCN2) in hepatic fibrosis. *Hepatol Res.* 2003;26(1):1–9.
  30. Zhao B, Ye X, Yu J, Li L, Li W, Li S, Yu J, Lin JD, Wang CY, Chinnaiyan AM, Lai ZC, Guan KL. TEAD mediates YAP-dependent gene induction and growth control. *Genes Dev.* 2008;22(14):1962–71.
  31. Vassilev A, Kaneko KJ, Shu H, Zhao Y, DePamphilis ML. TEAD/TEF transcription factors utilize the activation domain of YAP65, a Src/Yes-associated protein localized in the cytoplasm. *Genes Dev.* 2001;15(10):1229–41.
  32. Liu-Chittenden Y, Huang B, Shim JS, Chen Q, Lee SJ, Anders RA, Liu JO, Pan D. Genetic and pharmacological disruption of the TEAD-YAP complex suppresses the oncogenic activity of YAP. *Genes Dev.* 2012;26(12):1300–5.
  33. Tesmer JJ, Sunahara RK, Gilman AG, Sprang SR. Crystal structure of the catalytic domains of adenylyl cyclase in a complex with G $\alpha$ ph.GTP $\gamma$ S. *Science* 1997;278(5345):1907–16.
  34. Yamaguchi T, Pelling JC, Ramaswamy NT, Eppler JW, Wallace DP, Nagao S, Rome LA, Sullivan LP, Grantham JJ. cAMP stimulates the in vitro proliferation of renal cyst epithelial cells by activating the extracellular signal-regulated kinase pathway. *Kidney Int.* 2000;57(4):1460–71.
  35. Francis H, Glaser S, Ueno Y, Lesage G, Marucci L, Benedetti A, Taffetani S, Marziani M, Alvaro D, Venter J, Reichenbach R, Fava G, Phinizz JL, Alpini G. cAMP stimulates the secretory and proliferative capacity of the rat intrahepatic biliary epithelium through changes in the PKA/Src/MEK/ERK1/2 pathway. *J Hepatol.* 2004;41(4):528–37.
  36. Gurda GT, Zhu Q, Bai H, Devadason CA, Pan D, Schwarz KB, Anders RA. The utility of Yes-associated protein (YAP) expression in the diagnosis of persistent neonatal cholestatic liver disease. *Hum Pathol.* 2014;45(5):1057–64.
  37. Turkbey B, Ocak I, Daryanani K, Font-Montgomery E, Lukose L, Bryant J, Tuchman M, Mohan P, Heller T, Gahl WA, Choyke PL, Gunay-Aygun M. Autosomal recessive polycystic kidney disease and congenital hepatic fibrosis (ARPKD/CHF). *Pediatr Radiol.* 2009;39(2):100–11.
  38. Guay-Woodford LM. Autosomal recessive polycystic kidney disease: The prototype of the hepato-renal fibrocystic diseases. *J Pediatr Genet.* 2014;3(2):89–101.
  39. Jiang L, Fang PP, Weemhoff JL, Apte U, Pritchard MT. Evidence for a (pathogenic triumvirate) in congenital hepatic fibrosis in autosomal recessive polycystic kidney disease. *Biomed Res Int.* 2016.
  40. Liu F, Lagares D, Choi KM, Stopfer L, Marinkovic A, Vrbanc V, Probst CK, Hiemer SE, Sisson TH, Horowitz JC, Rosas IO, Fredenburgh LE, Feghali-Bostwick C, Varelas X, Tager AM, Tschumperlin DJ. Mechanosignaling through YAP and TAZ drives fibroblast activation and fibrosis. *Am J Physiol Lung Cell Mol Physiol.* 2015;308(4):L344–57.
  41. Zhao B, Wei X, Li W, Udan RS, Yang Q, Kim J, Xie J, Ikenoue T, Yu J, Li L, Zheng P, Ye K, Chinnaiyan A, Halder G, Lai ZC, Guan KL. Inactivation of YAP oncoprotein by the Hippo pathway is involved in cell contact inhibition and tissue growth control. *Genes Dev.* 2007;21(21):2747–61.
  42. Overholtzer M, Zhang J, Smolen GA, Muir B, Li W, Sgroi DC, Deng CX, Brugge JS, Haber DA. Transforming properties of YAP, a candidate oncogene on the chromosome 11q22 amplicon. *Proc Natl Acad Sci USA* 2006;103(33):12405–10.
  43. Zender L, Spector MS, Xue W, Flemming P, Cordon-Cardo C, Silke J, Fan ST, Luk JM, Wigler M, Hannon GJ, Mu D, Lucito R, Powers S, Lowe SW. Identification and validation of oncogenes in liver cancer using an integrative oncogenomic approach. *Cell* 2006;125(7):1253–67.
  44. Steinhart AA, Gayyed MF, Klein AP, Dong J, Maitra A, Pan D, Montgomery EA, Anders RA. Expression of Yes-associated protein in common solid tumors. *Hum Pathol.* 2008;39(11):1582–9.
  45. Wang KC, Yeh YT, Nguyen P, Limqueco E, Lopez J, Thorossian S, Guan KL, Li YJ, Chien S. Flow-dependent YAP/TAZ activities regulate endothelial phenotypes and atherosclerosis. *Proc Natl Acad Sci USA* 2016;113(41):11525–30.
  46. Gradilone SA, Habringer S, Masyuk TV, Howard BN, Masyuk AI, Larusso NF. HDAC6 is overexpressed in cystic cholangiocytes and its inhibition reduces cystogenesis. *Am J Pathol.* 2014;184(3):600–8.
  47. Masyuk TV, Radtke BN, Stroope AJ, Banales JM, Masyuk AI, Gradilone SA, Gajdos GB, Chandok N, Bakeberg JL, Ward CJ, Ritman EL, Kiyokawa H, LaRusso NF. Inhibition of Cdc25A suppresses hepato-renal cystogenesis in rodent models of polycystic kidney and liver disease. *Gastroenterology* 2012;142(3):622–33 e4.
  48. Cnossen WR, te Morsche RH, Hoischen A, Gilissen C, Christpijn M, Venselaar H, Mehdi S, Bergmann C, Veltman JA, Drenth JP. Whole-exome sequencing reveals LRP5 mutations and canonical Wnt signaling associated with hepatic cystogenesis. *Proc Natl Acad Sci USA* 2014;111(14):5343–8.
  49. Fabris L, Cadamuro M, Fiorotto R, Roskams T, Spirli C, Melero S, Sonzogni A, Joplin RE, Okolicsanyi L, Strazzabosco M. Effects of angiogenic factor overexpression by human and rodent cholangiocytes in polycystic liver diseases. *Hepatology* 2006;43(5):1001–12.

50. Spirli C, Okolicsanyi S, Fiorotto R, Fabris L, Cadamuro M, Lecchi S, Tian X, Somlo S, Strazzabosco M. Mammalian target of rapamycin regulates vascular endothelial growth factor-dependent liver cyst growth in polycystin-2-defective mice. *Hepatology* 2010;51(5):1778–88.
51. Gradilone SA, Masyuk TV, Huang BQ, Banales JM, Lehmann GL, Radtke BN, Stroope A, Masyuk AI, Splinter PL, LaRusso NF. Activation of Trpv4 reduces the hyperproliferative phenotype of cystic cholangiocytes from an animal model of ARPKD. *Gastroenterology* 2010;139(1):304–14. e2.
52. Spirli C, Morell CM, Locatelli L, Okolicsanyi S, Ferrero C, Kim AK, Fabris L, Fiorotto R, Strazzabosco M. Cyclic AMP/PKA-dependent paradoxical activation of Raf/MEK/ERK signaling in polycystin-2 defective mice treated with sorafenib. *Hepatology* 2012;56(6):2363–74.
53. Lu L, Li Y, Kim SM, Bossuyt W, Liu P, Qiu Q, Wang YD, Halder G, Finegold MJ, Lee JS, Johnson RL. Hippo signaling is a potent in vivo growth and tumor suppressor pathway in the mammalian liver. *Proc Natl Acad Sci USA* 2010;107(4):1437–42.
54. Lee KP, Lee JH, Kim TS, Kim TH, Park HD, Byun JS, Kim MC, Jeong WI, Calvisi DF, Kim JM, Lim DS. The Hippo-Salvador pathway restrains hepatic oval cell proliferation, liver size, and liver tumorigenesis. *Proc Natl Acad Sci USA* 2010;107(18):8248–53.
55. Song H, Mak KK, Topol L, Yun K, Hu J, Garrett L, Chen Y, Park O, Chang J, Simpson RM, Wang CY, Gao B, Jiang J, Yang Y. Mammalian Mst1 and Mst2 kinases play essential roles in organ size control and tumor suppression. *Proc Natl Acad Sci USA* 2010;107(4):1431–6.
56. Zhou DW, Conrad C, Xia F, Park JS, Payer B, Yin Y, Lauwers GY, Thasler W, Lee JT, Avruch J, Bardeesy N. Mst1 and Mst2 maintain hepatocyte quiescence and suppress hepatocellular carcinoma development through inactivation of the Yap1 oncogene. *Cancer Cell* 2009;16(5):425–38.
57. Ward CJ, Hogan MC, Rossetti S, Walker D, Sneddon T, Wang X, Kubly V, Cunningham JM, Bacallao R, Ishibashi M, Milliner DS, Torres VE, Harris PC. The gene mutated in autosomal recessive polycystic kidney disease encodes a large, receptor-like protein. *Nat Genet.* 2002;30(3):259–69.
58. Katsuyama M, Masuyama T, Komura I, Hibino T, Takahashi H. Characterization of a novel polycystic kidney rat model with accompanying polycystic liver. *Exp Anim.* 2000;49(1):51–5.
59. Masyuk TV, Huang BQ, Masyuk AI, Ritman EL, Torres VE, Wang XF, Harris PC, LaRusso NF. Biliary dysgenesis in the PCK rat, an orthologous model of autosomal recessive polycystic kidney disease. *Am J Pathol.* 2004;165(5):1719–30.
60. Schrader J, Gordon-Walker TT, Aucott RL, van Deemter M, Quaas A, Walsh S, Benten D, Forbes SJ, Wells RG, Iredale JP. Matrix stiffness modulates proliferation, chemotherapeutic response, and dormancy in hepatocellular carcinoma cells. *Hepatology* 2011;53(4):1192–205.
61. Low BC, Pan CQ, Shivashankar GV, Bershadsky A, Sudol M, Sheetz M. YAP/TAZ as mechanosensors and mechanotransducers in regulating organ size and tumor growth. *FEBS Lett.* 2014;588(16):2663–70.
62. Xiao Z, Quarles LD. Physiological mechanisms and therapeutic potential of bone mechanosensing. *Rev Endocr Metab Disord.* 2015;16(2):115–29.
63. Locatelli L, Cadamuro M, Spirli C, Fiorotto R, Lecchi S, Morell CM, Popov Y, Scirpo R, De Matteis M, Amenduni M, Pietrobattista A, Torre G, Schuppan D, Fabris L, Strazzabosco M. Macrophage recruitment by fibrocystin-defective biliary epithelial cells promotes portal fibrosis in congenital hepatic fibrosis. *Hepatology* 2016;63(3):965–82.
64. Verteporfin therapy of subfoveal choroidal neovascularization in age-related macular degeneration: Two-year results of a randomized clinical trial including lesions with occult with no classic choroidal neovascularization—verteporfin in photodynamic therapy report 2. *Am J Ophthalmol.* 2001;131(5):541–60.